AMERICAN SOCIETY FOR MICROBIOLOGY | mSphere

Editor's Pick | Bacteriology | Research Article

Acinetobacter enrichment shapes composition and function of the bacterial microbiota of field-grown tomato plants

Senga Robertson,[1] Alexandros Mosca,[1,2,3] Saira Ashraf,[1] Aileen Corral,[1] Rodrigo Alegria Terrazas,[1] Catherine Arnton,[1] Peter Thorpe,[2] Jenny Morris,[4] Pete E. Hedley,[4] Giulia Babbi,[5] Castrense Savojardo,[5] Pier Luigi Martelli,[5] Frederik Duus Møller,[6] Hanne Nørgaard Nielsen,[6] Pimlapas Leekitcharoenphon,[6] Frank M. Aarestrup,[6] Rashi Halder,[7] Cedric C. Laczny,[7] Paul Wilmes,[7,8] Laura Pietrantonio,[9] Pardo Di Cillo,[9] Vittoria Catara,[3] James Abbott,[2] Davide Bulgarelli[1]

AUTHOR AFFILIATIONS See affiliation list on p. 16.

ABSTRACT Tomato is a staple crop and an excellent model to study host-microbiota interactions in the plant food chain. In this study, we describe a "lab-in-the-field" approach to investigate the microbiota of field-grown tomato plants. High-throughput amplicon sequencing revealed a three-microhabitat partition, phyllosphere, rhizosphere, and root interior, differentiating host-associated communities from the environmental microbiota. An individual bacterium, classified as *Acinetobacter* sp., emerged as a dominant member of the microbiota at the plant-soil continuum. To gain insights into the functional significance of this enrichment, we subjected rhizosphere specimens to shotgun metagenomics. Similar to the amplicon sequencing survey, a "microhabitat effect," defined by a set of rhizosphere-enriched functions, was identified. Mobilization of mineral nutrients, as well as adaptation to salinity and polymicrobial communities, including antimicrobial resistance genes (ARGs), emerged as a functional requirement sustaining metagenomic diversification. A metagenome-assembled genome representative of *Acinetobacter calcoaceticus* was retrieved, and metagenomic reads associated with this species identified a functional specialization for plant-growth promotion traits, such as phosphate solubilization, siderophore production, and reactive oxygen species detoxification, which were similarly represented in a tomato genotype-independent fashion. Our results revealed that the enrichment of a beneficial bacterium capable of alleviating plant abiotic stresses appears decoupled from ARGs facilitating microbiota persistence at the root-soil interface.

IMPORTANCE Tomatoes are at center stage in global food security due to their high nutritional value, widespread cultivation, and versatility. Tomatoes provide essential vitamins and minerals, contribute to diverse diets, and support farmer livelihoods, making them a cornerstone of sustainable food systems. Beyond direct dietary benefits, the intricate relationship between tomatoes, their associated microbiota, and antimicrobial resistance gene (ARG) is increasingly recognized. Tomato plants host diverse microbial communities in association with their organs, which influence plant health and productivity. Crop management impacts the composition and function of these communities, contributing to the prevalence of ARGs in the soil and on the plants themselves. These genes can potentially transfer to human pathogens, posing a food safety and public health risk. Understanding these complex interactions is critical for developing sustainable agricultural practices capable of mitigating the impact of climatic modifications and the global threat of antimicrobial resistance.

KEYWORDS food-chain microbiota, tomato, metagenomics, AMR, One Health

Editor Raffaele Zarrilli, Universita degli Studi di Napoli Federico II, Naples, Italy

Address correspondence to Davide Bulgarelli, d.bulgarelli@dundee.ac.uk.

Senga Robertson and Alexandros Mosca contributed equally to this article. Author order was determined based on seniority.

The authors declare no conflict of interest.

See the funding table on p. 17.

Received 2 December 2025
Accepted 11 December 2025
Published 15 January 2026

Plants host diverse microbial communities in association with their organs, collectively referred to as the plant microbiota. Similar to the microbiota inhabiting vertebrates, the plant microbiota modulates the growth, development, and health of its host (1). For instance, the microbiota at the root-soil continuum controls mineral biogeochemical cycles which, in turn, determine food provision as well as the environmental footprint of crop production (2). The plant microbiota does not represent a random assembly from the environment. Rather, a series of deterministic checkpoints define composition and function of the microbial assemblages thriving in association with plants (3). Consequently, the characterization of the plant microbiota gained center stage as a first step toward the identification and development of "probiotics" for plants (4).

In recent years, plant-associated microbes have emerged as a neglected reservoir for antimicrobial resistance mechanisms (5). Studies conducted with vascular plants and mosses identified antimicrobial resistance genes (ARGs) as microbiota determinants for host colonization (6, 7). As ARGs are embedded in the microbiota at the plant-soil continuum (8), it is critical to define their dynamics across plant species to inform strategies aimed at improving ecosystem functioning and One Health (9).

Cultivated tomato (*Solanum lycopersicum*) is a staple crop (10) and an excellent experimental model for dissecting the genetic bases of plant-environment interactions (11). As tomato production is threatened by climatic modifications on a global scale (12), it is not surprising that innovative strategies to strengthen environmental resilience have been proposed, including an example of *de novo* domestication, whereby genome editing has been used to "convert" a wild relative into a cultivated form (13). Among those strategies, the microbiota has gained center stage in both basic science and translational application as an untapped resource for climate change adaptation in crops (14), including tomato. For instance, the availability of tomato genetic resources enabled scientists to precisely identify host genetic determinants of the microbiota (15). Likewise, the threat posed by devastating soil-borne diseases has sparked efforts to identify a protective microbiota capable of fending off pathogens (16, 17). Despite the growing scientific interest in the tomato microbiota, available information remains focused on taxonomic investigations (18). Predictive approaches to infer function from community composition have been applied (19–21), yet examples of characterization of the tomato microbiota functional potential from soil-grown plants remain limited (22).

In this study, we embarked on a lab-in-the-field approach where, by sampling actual production sites in the Mediterranean environment, we determined a "plant footprint" on the composition and function of the tomato bacterial microbiota, which emerged sufficiently stable between the tested genotypes. Motivated by the discovery of an unusual dominance of an individual phylotype classified as *Acinetobacter* sp., we further investigated the implications for agriculture, including ARG dynamics for One Health.

MATERIALS AND METHODS

Soil, plant, and environmental samples

Sampling was performed in the summer of 2019 on a tomato farm close to the town of Larino (41°48′N, 14°55′E), in the south of Italy. The farm grows distinct, processing-type tomato F1 commercial hybrids: Abbundo (HM Clause; hereafter "Ab") and SV5197TP (Bayer; hereafter "SV"). Plants were maintained in distinct fields of soils displaying comparable chemical and physical composition (Table S1). Individual plantlets were transplanted in May, and sampling was performed in mid-June at the early flowering stage by uprooting individual plants (Fig. S1). Inter-row soil was used as "unplanted control" representing the "bulk soil" microhabitat. Samples were sealed in plastic bags and transported refrigerated to the University of Dundee. Crop management was identical for both hybrids, and no significant difference in yield was recorded between hybrids (Pardo DiCillo, personal communication).

Sample preparation and DNA extraction

Upon arrival, individual plants were shaken vigorously to remove any excess soil and debris. The resulting specimen of roots and rhizosphere soil was transferred to a 50 mL sterile falcon tube containing 15 mL phosphate-buffered saline solution (PBS). Rhizosphere was extracted by vortexing for 30 s; samples were then transferred to a second falcon tube containing 15 mL PBS, and the process was repeated to maximize rhizosphere recovery. The roots were removed from the sample tube and stored in a third PBS-containing tube on ice for downstream preparation the same day. The rhizosphere suspensions were combined and centrifuged at 1,500 × *g* for 20 min to pellet the rhizosphere; the PBS supernatant was discarded, and the pellet was flash frozen using liquid nitrogen. Roots were removed from PBS storage and placed in sterile mortars, flash frozen with liquid nitrogen, and finely crushed using a sterile pestle. Powdered root material was transferred to a sterile 15 mL falcon tube and flash frozen in liquid nitrogen. Leaf material was gently washed with sterile water and subjected to the same fine-crushing protocol as described for root samples.

Unplanted soil was processed in a similar way to rhizosphere samples; 2 g–3 g of bulk soil was transferred to a sterile 50 mL falcon tube containing 15 mL PBS and subjected to the same centrifugation, supernatant disposal, and flash freezing process.

All processed unplanted, rhizosphere, root, and leaf samples were stored at −70°C until further analysis. Each sample was subjected to DNA extraction using the FastDNA SPIN Kit for Soil (MP Biomedicals, Solon, USA) according to the manufacturer's instructions.

Six replicated swabs obtained from non-contiguous areas of each farm machinery used prior to tomato harvesting and including two tractors, two water hoses, a cultivator, a herbicide dispenser, and the harvester were subjected to DNA extraction using the PowerSoil Pro kit (Qiagen, Manchester, UK) according to the manufacturer's instructions.

Amplicon preparation and sequencing

For bacterial amplicon profiling, the 16S rRNA hypervariable V4 region of the small ribosomal subunit rRNA gene was subjected to targeted amplification using the primer pair 515F (5′-GTGCCAGCMGCCGCGGTAA-3′) and 806R (5′-GGACTACHVGGGTWTCTAAT-3′). The forward primers incorporate the Illumina flow cell adapter sequence at the 5′ termini, and the reverse primers include unique 12 bp indexes incorporated to allow for multiplexing (23). 16S rRNA gene PCR amplification was conducted using the KAPA HiFi Hotstart PCR Kit (KAPA Biosystems, Wilmington, USA). Metagenomic DNA (50 ng per sample) was used and individual reactions consisted of 4 µL 5× KAPA HiFi Buffer, 1 µL 10 mg/mL bovine serum albumin, 0.6 µL 10 mM dNTPs, 0.6 µL 10 µM forward primer, 0.6 µL 10 µM reverse primer, 0.25 µL KAPA HiFi polymerase, 2 µL 5 µM pPNA chloroplast blocker, 2 µL 5 µM mPNA mitochondrial blocker (24). The reactions were amplified using the following program: 94°C (3 min), followed by 35 cycles of 98°C (30 s), 50°C (30 s), and 72°C (1 min), followed by a final single step of 72°C (10 min). For each sample/index combination, a no-template control (NTC) was run containing no DNA.

PCRs were performed in triplicate and using at least two individual master mix plates, equating to six replicates per sample, to minimize amplification biases. PCR reactions were pooled in an index-wise manner, and 5 µL of each sample was run on 1.5% agarose gel alongside its corresponding NTC. Only samples with clear banding at around 450 bp and where there was no detectable amplification of the corresponding NTC were taken forward. Amplicons were purified using Agencourt AMPure XP beads (Beckman Coulter, Amersham, UK) at a ratio of 0.7 µL beads to 1 µL sample. Individually indexed samples were pooled together in an equimolar ratio, supplemented with 20% PhiX control library, and run as recommended at a final concentration of 4 pM on an Illumina MiSeq with 2 × 150 bp chemistry. Sequencing of farm machinery-derived metagenomic DNA was performed as previously described (25). Briefly, ~5 ng of isolated DNA was used for PCR amplification using primer pair 341F (5′-CCTACGGGNGGCWGCAG-3′) and 785R (5′-GACTACHVGGGTATCTAATCC-3′). An overhang adapter sequence was added in

both primers. A second PCR was performed with primers against overhang sequences containing 8 bp combinatorial dual indexes using product from the first PCR as template. The purified second PCR product was pooled in equimolar concentration and was sequenced on a MiSeq using 2 × 300 bp paired-end reads.

Amplicon data processing

Sequencing read quality was assessed using FastQC, then DADA2 and R were used to generate ASV-count matrices using the basic methodology as outlined in the DADA2 pipeline tutorial, as previously described (26). Briefly, read filtering was conducted using the DADA2 paired FastqFilter method, trimming 10 bp of sequence from the 5′ end of each read using a truncQ parameter of 2 and the maximum number of "expected" errors in a read of 2. The majority of amplicon reads remaining after this process were of high quality and did not require 3′ end trimming. The DADA2::Learn_errors() method was run to determine the error model with a MAX CONSIST parameter of 20, whereby the error model will converge or be close to convergence within 20 rounds. The DADA2::DADA() method was then run with the error model to de-noise the readings using sample pooling. Reads were then merged, setting a minimum overlap of 12 bp (actual overlap in the final amplicon pool 45 bp–49 bp) followed by the removal of chimeras using the consensus method. The dada2::assignTaxonomy() method was used using the RDP Naïve Bayesian Classifier to assign taxonomy with the SILVA database version 138 (27) imposing a minimum bootstrap confidence of 50. Following taxonomic assignment, the outputs were converted into "phyloseq objects" (27) for downstream statistical analyses and figure generation. The phyloseq object was pruned *in silico* of ASVs classified as chloroplast and mitochondria as well as matching a data set of putative contaminants of the lab (28). Likewise, we discarded ASVs for which we were unable to determine affiliation at the phylum level. Next, we imposed a secondary quality filtering (29) based on ASV abundance, retaining in the final data set only those accruing 20 reads in at least 1% of the samples (i.e., an individual sample or more). Following pre-processing, samples with more than 5,000 reads were retained for downstream analysis. Rarefaction curves were computed with the R package vegan using a pre-compiled code (30) while ecological indices, that is, alpha and beta diversity, were computed with phyloseq. Upon assessing data distribution with a Shapiro-Wilk test, univariate statistical analysis was performed using either analysis of variance or a Kruskal-Wallis test, setting an alpha level of 0.05. Permutational analyses of variance on distance matrices were computed using the function adonis of the package vegan (31). We used DESeq2 (32) to identify differential enrichments, as previously described (26).

Co-occurrence networks

Co-occurrence networks were generated using ASV data agglomerated at the genus level. Briefly, networks were generated with SparCC (33), considering only genera with a relative abundance greater than 0.05% and occurring in at least 50% of the samples in the set. Cytoscape (34) was adopted to visualize and analyze networks. Both positive and negative correlations with an absolute value greater than or equal to 0.50 were plotted in networks, but only positive correlations have been retained to analyze network modularization. The Cytoscape GLay plugin (35) was used to identify modules—that is, groups of nodes more tightly connected among each other than with the rest of the network. The NetworkAnalyzer plugin (36) was used to identify central genera. Three different centrality measures, that is, degree, betweenness, and closeness, were computed for each node in a network (36). For each network, the distributions of node centralities were computed independently for each measure. Nodes with at least one measure higher than the 90th percentile were retained as central.

Metagenomic data preparation and sequencing

Raw DNA samples (70 µL) were purified using the Agencourt AMPure XP Kit with a ratio of 1.8 µL beads per 1 µL sample. The samples were eluted in Buffer EB with a final

volume of 40 µL, and their concentration was measured by Qubit. The samples were then fragmented using QIAGEN FX DNA Library Core Kit. One hundred ten nanograms of sample was fragmented in a total volume of 50 µL including 5 µL 10× FX Buffer and 10 µL FX Enzyme Mix. Fragmentation was performed in a thermocycler using the following program: 4°C for 1 min, 32°C for 6 min (varies with amount of DNA), 65°C for 30 min, and finally holding sample at 4°C. For samples with less than 110 ng of DNA, the FX reaction mix was made to a total volume of 60 µL with 6 µL 10× FX Buffer and 12 µL FX Enzyme Mix. The fragmentation time at 32°C was also varied according to the amount of DNA as follows: 60 ng–100 ng DNA – 7 min; 40 ng–60 ng DNA – 8 min; 20 ng–40 ng DNA – 9 min. Each sample had a unique adapter attached, which allowed binding to the Illumina flow cell for sequencing purposes and the unique identification of the samples in the library. The QIAseq UDI Y-Adapter Kit was used, and 5 µL of a unique adapter was added per sample. Subsequently, 20 µL 5× Ligation Buffer, 10 µL DNA ligase, and either 15 or 5 µL nuclease-free water were added per sample, depending on the volume of the fragmented sample, to make a total volume of 100 µL. The fragmented samples were then incubated at 20°C for 15 min in a thermocycler with the heated lid off. Immediately afterward, the samples were cleaned up using 0.8× (80 µL) Agencourt AMPure XP beads and eluted in 52.5 µL of Buffer EB. A second purification was performed using 1× (50 µL) Agencourt AMPure XP beads and eluted in 26 µL Buffer EB. After adapter ligation and sample purification, PCR amplification was performed on the DNA samples. To 23.5 µL sample DNA, 25 µL QIAseq 2× HiFi PCR Master Mix and 1.5 µL QIAseq Primer Mix (10uM each) was added. PCR was then performed in a thermocycler using the following program: 98°C for 2 min, followed by 10 cycles of 98°C for 20 s, 60°C for 30 s, and 72°C for 30 s, and finally 72°C for 5 min before holding samples at 4°C. After performing PCR, the samples were purified using 1× (50 µL) Agencourt AMPure XP beads and eluted in 25 µL Buffer EB. The samples were checked for amplification by gel electrophoresis. Five microliters of each sample was run on a 1.5% agarose gel. A fragmented pattern with the highest intensity centered at around 550 bp indicated successful amplification. The DNA samples were then quantified using the Qubit 4 Fluorometer. An equimolar library was prepared and submitted for sequencing purposes. Metagenomics libraries were sequenced on an Illumina NextSeq 2000 instrument using a P3 kit (360 Gb) according to manufacturer's recommendations.

Metagenomic data processing

Sequencing reads were quality assessed using FastQC and quality/adapter trimmed using TrimGalore (37), using a quality cutoff of 20, a minimum sequence length of 100 bp, and removing terminal N bases. Taxonomic classification of the sequence reads was performed using Kraken 2.0.9 (38), with custom Kraken database consisting of the Kraken archaea, bacteria, plasmid, viral, human, fungi, plant, and protozoa sections. Host contamination was removed by alignment against the tomato cultivar Heinz 1706 (AEKE03000000) genome sequences, using BWA MEM (39), and non-aligning reads were extracted from the resulting BAM files using SAMtools (40). Metagenome assembly was conducted using MEGAHIT version 1.2.9 (41) with the "meta-large" preset. Metagenome-assembled genomes (MAGs) were created using the MEGAHIT-assembled contigs described above and MetaBAT2 version 2.15 (42) to create contig bins representing single genomes. Contig bins were dereplicated using dRep version 3.2.0 (43) followed by decontamination with MAGpurify version 2.1.2 (44). The resulting MAGs were assessed for completeness and contamination using CheckM (45). Annotation of the MAGs was performed with Bakta version 1.9 (46) before taxonomic classification was determined using the Genome Taxonomy Database Toolkit version 1.4.0 (47) with data version r95. To refine MAGs' identification, the processes of assembly, binning, and taxonomic identification were iteratively refined in two steps, conducted separately for both genotypes. In the first step, metagenomic reads were assembled after removing plant-derived sequences. In the second step, the remaining reads—that is, those not included in the previous assembly—were reassembled. Using BWA MEM and SAMtools,

the *Acinetobacter calcoaceticus* MAG was mapped against metagenomic reads that had been previously filtered to remove host sequences and the assembled reads from the first assembly.

Metagenomic reads classified as *Acinetobacter calcoaceticus* by Kraken 2.0.9 were extracted and subsequently indexed and mapped against the metagenomic data set using BWA, applying the default parameters for minimum seed length (19) and minimum alignment score (30). The aligned metagenomic reads were assessed using the "flagstat" command of SAMtools for the read alignment statistics, considering the only primary mapped reads of *A. calcoaceticus* on the metagenomic data set. To further validate the taxonomic classification, we performed an average nucleotide identity (48) comparison in Proksee (49) with the reference genomes of *A. calcoaceticus* (strain NCTC 12983; accession number PRJEB6403) and *A. baumannii* (strain ATCC 19606; accession number PRJNA557095) obtained from NCBI genome. PGPg_Finder (v.1.10) (50), based on the comprehensive PLaBAse tool version 1.01 (51), was used with the "metafast_wf" set in order to uncover the plant-growth promoting traits in the metagenomic sequences obtained from the remaining reads prior to the second assembly analysis and in the metagenomics reads of *Acinetobacter calcoaceticus*. PGPg_Finder outputs were converted into a phyloseq object for statistical analysis and figure generation (alpha, beta diversity, and differential enrichment analysis, see above). Individual samples were rarefied at 400,000 reads prior to calculation.

The additional assembled contigs have been mapped across the 37 samples using the jgi_summarize_bam_contig_depths command from MetaBat2, in order to estimate contig coverage in each sample. The gene functions of the contigs were then annotated using eggNOG-mapper (v.2.1.10) (52). Subsequently, the resulting data were considered to perform a functional enrichment analysis with DESeq2, comparing the functional profiles of the rhizosphere and soil separately for "Ab" and "SV" genotypes.

Resistome reconstruction and visualization

Metagenomics reads, quality checked and pruned of putative host contamination (see above), were mapped to whole-genome bacterial database from NCBI and ResFinder (53) for ARG using KMA alignment (54) and default parameters. ARG abundance was identified as FPKM (fragments per kilobase per million fragments). This accounted for both sample-wise sequencing depth differences and size-dependent probability of observing a reference (55). FPKM was calculated by first normalizing for read depth by dividing the read counts by the total number of reads aligned to the bacterial database in the sample, using a scaling factor of 1 million. Then, the read counts were normalized according to gene length by dividing them by the length of the gene in kilobases (56). For heatmap construction we used genes log(FPKM) values to narrow the range and enhance heatmap readability. Using the "vegdist" function from the Vegan R package, a distance matrix was generated based on Bray-Curtis dissimilarity, which quantifies differences between samples based on FPKM values. Sample clustering was executed using the "pheatmap()" function from the pheatmap R package, employing complete linkage hierarchical clustering on the Bray-Curtis distance matrix.

The reconstructed *Acinetobacter* MAG was submitted to the public ResFinder server and the Comprehensive Antibiotic Resistance Database – Resistance Gene Identifier (57) for ARG identification using default and "stringent" parameters, respectively.

Acinetobacter genomes phylogenetic analysis

We retrieved 67 publicly available *Acinetobacter calcoaceticus* genomes and categorized them as "plants/soil" or "other" according to isolation source information available on NCBI. Phylogenetic tree construction and annotation was performed as previously described (58).

RESULTS

The bacterial microbiota of field-grown tomato plants is a "gated" community

We generated 173 bacterial 16S rRNA gene amplicon profiles of four microhabitats, that is, unplanted soil, rhizosphere, roots, and leaves, from two tomato F1 hybrids grown in adjacent fields in the south of Italy. Upon *in silico* pruning of ASVs putatively representing host or environmental contamination and applying an abundance threshold, we retained 129 samples: number of samples unplanted soil $N_{unplanted}$ = 14; $N_{rhizosphere}$ = 51; N_{roots} = 49; N_{leaves} = 15. Those samples accrued for 940 ASVs and 3,747,178 sequencing reads. These ASVs were affiliated with 20 phyla, although 5, namely Acidobacteriota, Actinobacteriota, Bacteroidota, Firmicutes, and Proteobacteria, represented over 99% of the retained reads in plant-associated microhabitats (Fig. S2).

Rarefaction curves indicated that we reached a plateau-like pattern for the vast majority of our samples (Fig. S3), motivating us to inspect ASV richness and evenness across microhabitats. This revealed a distinct pattern for the tomato bacterial microbiota, manifested by a significant reduction in both metrics when comparing plant-associated microhabitats, that is, leaves, roots, and rhizosphere, with unplanted soil controls (Fig. 1A and B; Kruskal-Wallis test, individual *P*-values <0.05). Likewise, a dissimilarity matrix computed on microbiota composition partitioned individual samples in a microhabitat-dependent manner (Fig. 1C, R^2 "Microhabitat" = 0.52, adonis test, *P*-value <0.001; 5,000 permutations).

To gain further insights into the individual members of the microbiota underpinning the compositional diversification, we took a two-pronged approach. First, we generated co-occurrence networks computed on bacterial genera relative abundance. Outputs of this investigation mirrored the previously identified pattern: while unplanted samples returned ten modules, plant-associated microhabitats were characterized by only three or four (Fig. 2). Likewise, network topology, defined by the number of nodes and edges, emerged as more complex in unplanted soil compared to plant-associated microhabitats (Table S2). A further discrimination emerged from the taxonomic inspection of these networks: in unplanted soil and leaves, the group *Allorhizobium-Neorhizobium-Pararhizobium-Rhizobium* was more central than in roots and rhizosphere microhabitats. Conversely, belowground networks appeared supported by other Proteobacteria and Firmicutes (Table S2).

Next, we performed pair-wise comparisons between unplanted soil with root and rhizosphere specimens, respectively. We identified ASVs significantly enriched in and diagnostic for plant-associated microhabitats, although their numbers appeared orders of magnitude lower than what previously reported for the species (18) (Fig. 3, Wald test, individual *P*-values <0.05; FDR corrected; see Data Set S1 at https://zenodo.org/records/17580416). Closer inspection revealed that an individual ASV, classified as *Acinetobacter* sp., accrued for ~30% of sequencing reads on average in both root and rhizosphere specimens, regardless of the genotype investigated (Fig. S4). Since a dominant *Acinetobacter* is likely to occupy niches that would otherwise be available to other members of the microbiota, this may explain, at least in part, the reduced number of observations compared with other studies.

This surprisingly high proportion of an individual bacterium motivated us to inspect the microbiota composition of seven farm machineries as possible sources of an artificially derived *Acinetobacter* contamination. Although different amplification protocols prevented us from performing a deeper taxonomic comparison, the resulting farm machinery microbiota was dominated by members of the phylum Actinobacteriota (mean read proportion ~39% across samples; Fig. S5). Conversely, *Acinetobacter* sp. was detected at the same order of magnitude of bulk soil specimens (mean read proportion ~1.5% across samples; Fig. S5). We therefore concluded that the observed *Acinetobacter* dominance represents a *bona fide* endogenous trait of the field-grown tomato microbiota.

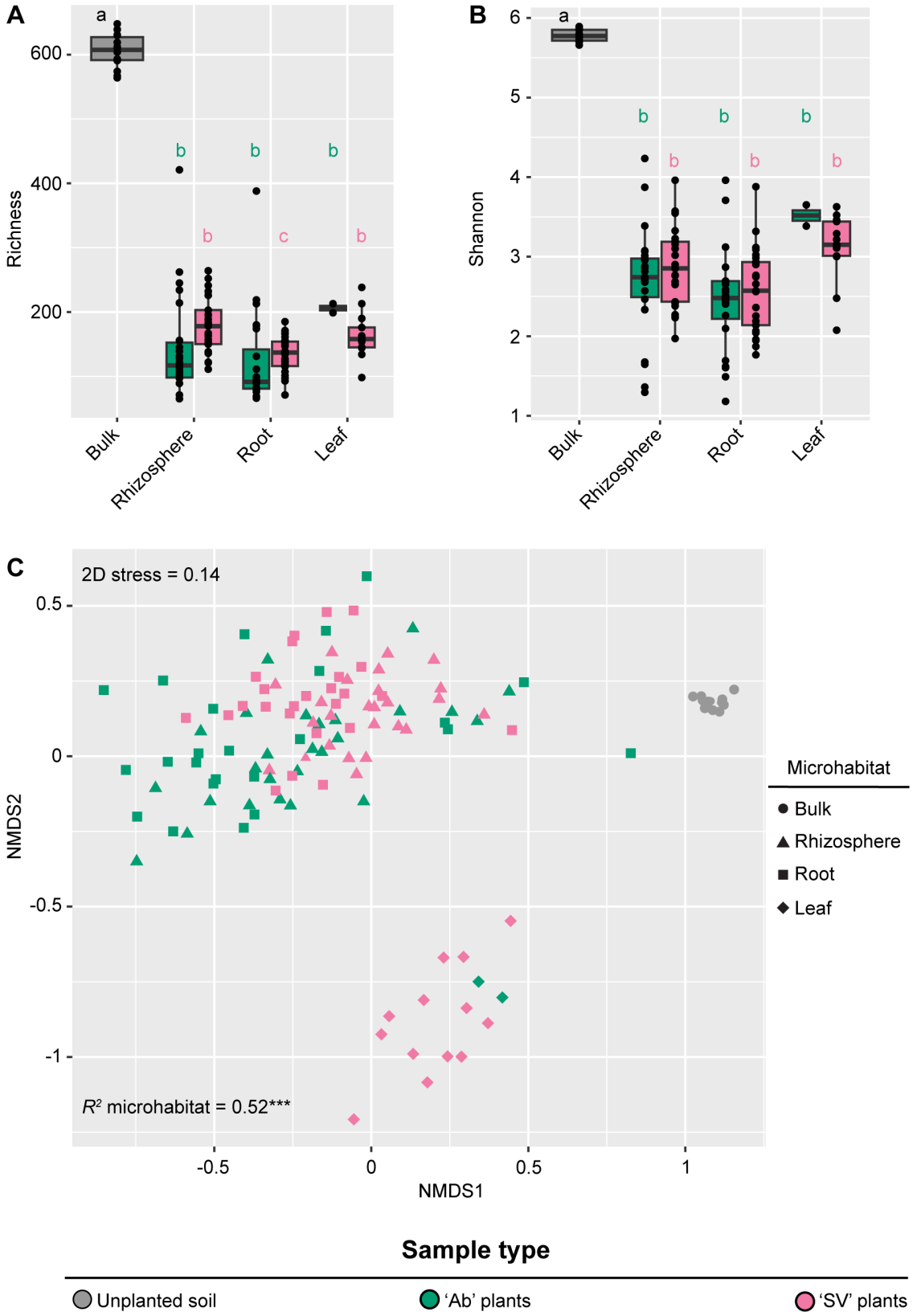

FIG 1 (A) Total number of observed ASVs and (B) Shannon's diversity index, calculated for bulk and plant-associated microhabitats. The upper and lower edges of the box plots represent the upper and lower quartiles, respectively. The bold line within the box denotes the median; individual shapes depict measurements of individual biological replicates/genotypes for a given microhabitat. Different letters denote statistically significant differences between microhabitat means

(Continued on next page)

Fig 1 (Continued)

by Kruskal-Wallis non-parametric analysis of variance followed by Dunn's *post hoc* test (individual *P*-values <0.05; BH corrected). (C) Nonmetric multidimensional scaling computed using a Bray-Curtis dissimilarity matrix. Individual shapes depict replicates of the indicated microhabitats, color-coded according to sample type or genotype. The R^2 value depicts the proportion of variation in distances explained by the factor microhabitats (adonis test, asterisks denote *P*-value <0.001; 5,000 permutations).

A three-pronged functional specialization of the tomato rhizosphere bacterial microbiota

To gain insights into the functional significance of the bacterial microbiota for field-grown tomato plants, we reconstructed 37 bulk soil and rhizosphere metagenomes and classified ~675 million paired-end reads. Taxonomic profiles of metagenomic samples were dominated by bacteria (>637 million reads, ~94% classified reads; see Data Set S2 at https://zenodo.org/records/17580416) and mirrored the ones obtained from cognate amplicon samples and returned a limited, but significant, correlation between the two methodologies (Fig. S6; Spearman's rank correlation rho = 0.17; *P*-value = 0.0003). This observation suggests that the footprint of host selection at the root-soil interface is sufficiently resistant to sequencing bias.

This motivated us to mine a repository of plant-growth promoting traits (59) to determine functional specializations of the tomato rhizosphere microbiota. This allowed us to identify 2,642 individual microbial genes putatively representing plant growth-promoting traits. Inspection of gene distribution between microhabitats revealed an opposite trend compared to amplicon sequencing profiles. Irrespective of the plant genotype tested, the rhizosphere microhabitat emerged with richer and more diverse functional profiles than bulk soil controls (Fig. 4A and B; Kruskal-Wallis test, individual *P*-values <0.05) while functional gene abundance returned a clear microhabitat-dependent partition of individual samples (Fig. 4C, R^2 "Microhabitat" = 0.68, adonis test, *P*-value <0.001; 5,000 permutations). This apparent incongruence between microbial richness can be explained by the fact that plant-growth-promoting traits are likely to be enriched in plant-associated samples compared to unplanted controls. Consistently, the rhizosphere enrichment of 15 functional categories out of 142 accrued for over half the sequencing reads and significantly discriminated between microhabitats (Fig. 4D, Wald test, individual *P*-values <0.05; FDR corrected; see Data Set S3 at https://zenodo.org/records/17580416). These functional categories defined a three-pronged specialization of the tomato microbiota: alongside genes required for the mobilization and plant uptake of mineral nutrients, we identified genes putatively implicated in adaptation to abiotic stresses as well as modulation of inter-organismal relationships. Among the latter, we identified genes putatively implicated in antimicrobial resistance. We therefore reconstructed a resistome representative of the metagenomic data set. We were able to identify 25 ARGs with sufficient confidence. Although we did not discern clear microhabitat- or genotype-dependent patterns, genes coding for beta-lactamase emerged as dominating the sequencing profiles (12 out of 25 identified genes; Fig. 5).

Plant-growth promoting functions of *A. calcoaceticus* are stable between host genotypes

To further investigate the potential plant-growth promotion traits (PGPTs) of the dominant member of the bacterial communities, we attempted to reconstruct MAGs phylogenetically related to *Acinetobacter* sp., a strategy successfully applied to study the genomic diversity of *Acinetobacter* from "unconventional" sources (60–62). First, we assembled over 1.5 Gbp metagenomic reads from the two tomato genotypes (Table S3) from which we were able to reconstruct an individual *Acinetobacter* sp. MAG with completeness >70% and contamination <10%, taxonomically identified as *Acinetobacter calcoaceticus*. Comparison of the MAG sequences with the reference genome of *A. calcoaceticus* returned an average nucleotide identity of 94.99%, greater than the value of 86% obtained when the same analysis was performed against the reference genomes

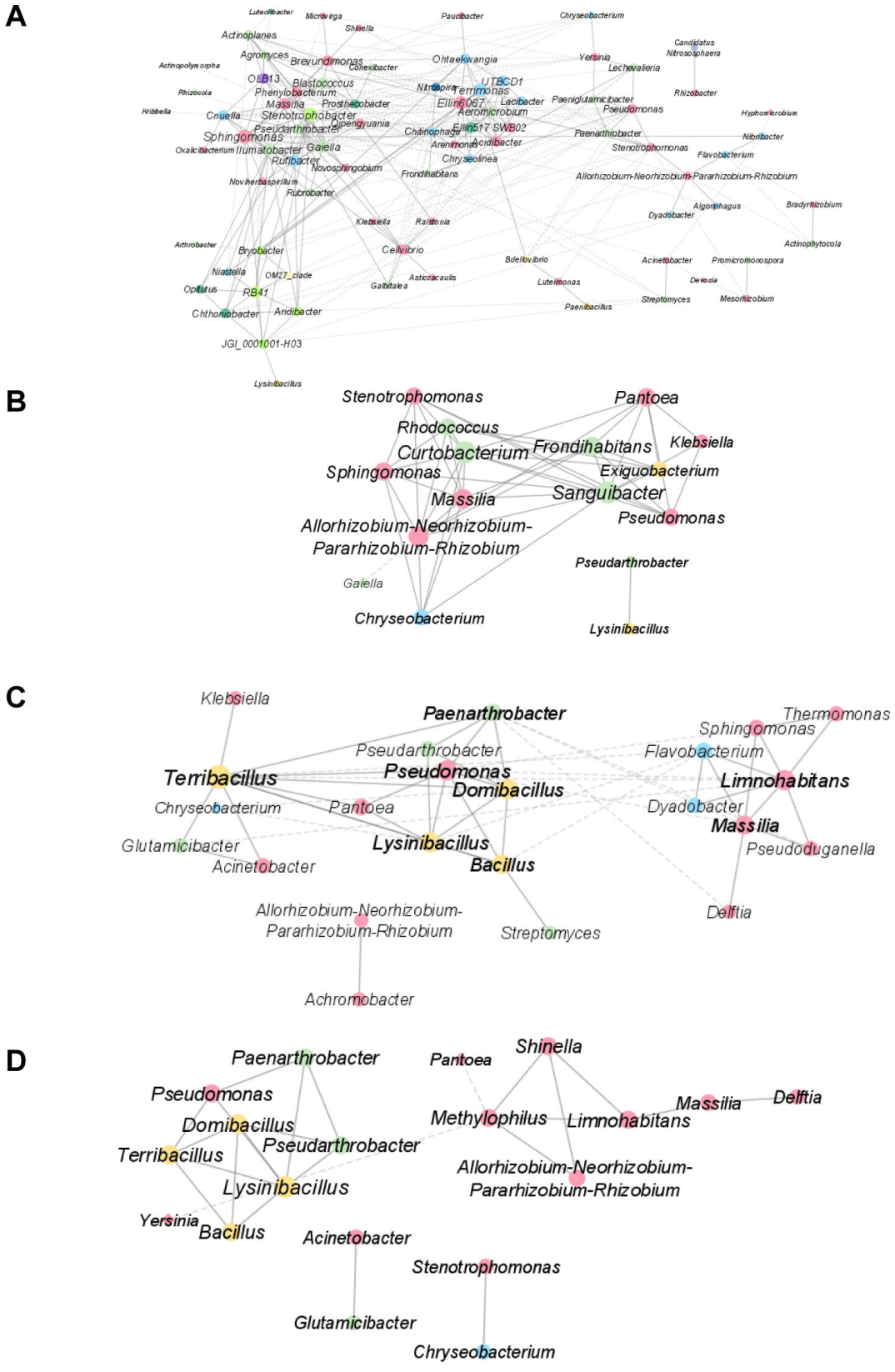

FIG 2 Correlation networks among bacterial genera for bulk (A), leaves (B), rhizosphere (C), and root (D) samples. Nodes are colored following the bacterial phylum. Links depicted with solid lines and dashed lines represent positive and negative correlations, respectively. Node dimensions are proportional to the node degree.

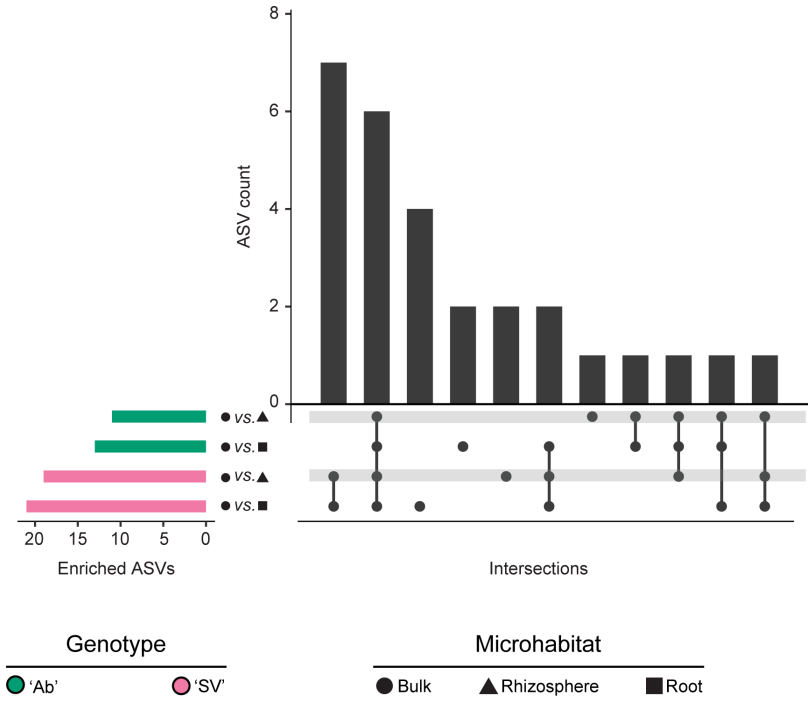

FIG 3 Horizontal blue bars denote the number of ASVs differentially enriched (Wald test, individual *P*-values of <0.05, FDR corrected) between the bulk soil and root and rhizosphere microhabitats in the two tomato genotypes, as recapitulated by the shape and color scheme. Vertical bars depict the number of differentially enriched ASVs unique to or shared among two or more pairwise comparisons highlighted by the interconnected dots underneath the vertical bars.

of *A. baumannii*. This motivated us to retrieve 67 publicly available *A. calcoaceticus* genomes to inspect phylogenetic relatedness and colonization preference within the species. Although no clear partition according to ecological niche could be discerned, we identified two plants/soil isolates among the closest relatives of the identified MAG (Fig. S7). This further supports the notion that the *Acinetobacter* dominance of the amplicon and metagenomic profiles may represent an endogenous colonization of the field-grown tomato microbiota. Mapping analysis of the *A. calcoaceticus* MAG against the metagenomic reads, filtered to exclude plant host sequences and previously assembled reads, revealed a similar representativeness of this bacterial species across the two genotypes. In line with the ASV data, the prevalence of the mapped reads was in the rhizosphere samples, indicating a high representativeness of this MAG in specific "Ab" rhizosphere samples, with the highest proportion of more than 10% among them (Table S4).

However, when we explored the abundance of PGPTs extracted from *A. calcoaceticus* reads, no host-genotype effect was identified (Wald test, individual *P*-values >0.05, FDR corrected). In both genotypes, among over 2.8 million gene abundances in 2,545 genes, at least 50% of the genes were included in pathways within the "Biofertilization," "Colonizing plant system," "Biocontrol," "Competitive exclusion," "Bioremediation," and "Phytohormone and Plant Signaling" categories (Fig. 6A and B; see Data Set S4 at https://zenodo.org/records/17580416). Regardless of the host genotype, the PGPTs associated with *A. calcoaceticus* metagenomic reads were mostly represented by functions related to organic acid metabolism and ROS scavenging, involved in phosphate assimilation and biocontrol activities, respectively. Despite the functional conservation among tomato genotypes (Fig. 6; see Data Set S4 at https://zenodo.org/records/17580416), ~10% PGPTs were uniquely identified in "Ab" and "SV" *Acinetobacter* MAG profiles, representing a possible "footprint" of host selection on the rhizosphere microbiota (Fig. S8; see Data Set S4 at https://zenodo.org/records/17580416). We next mined for ARGs in the *Acinetobacter* MAG: intriguingly, we failed to identify significant "hits" in multiple

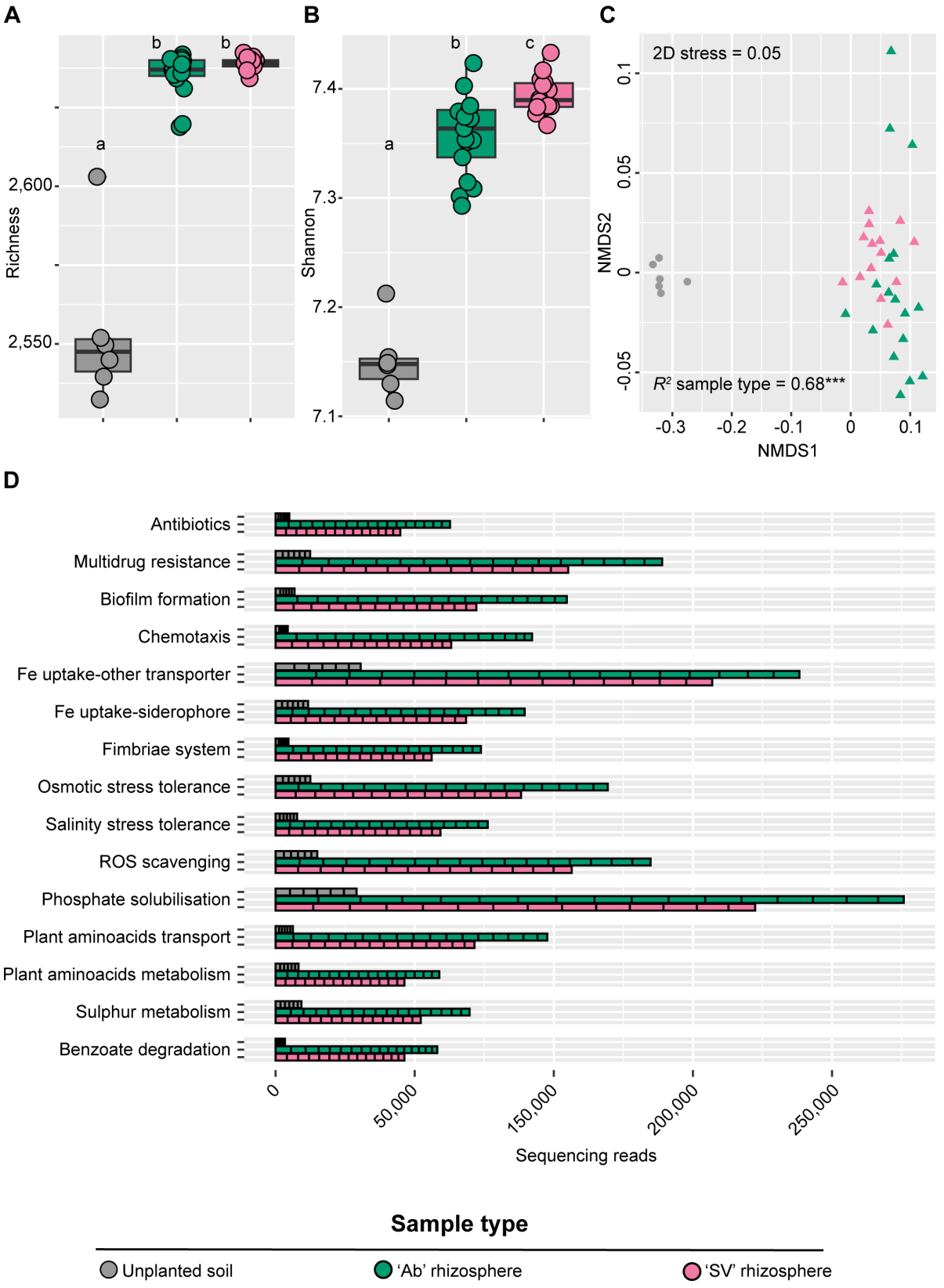

FIG 4 (A) Total number of observed functions and (B) Shannon's diversity index, calculated for bulk and rhizosphere microhabitats. The upper and lower edges of the box plots represent the upper and lower quartiles, respectively. The bold line within the box denotes the median; individual shapes depict measurements of individual biological replicates/genotypes for a given microhabitat. Different letters denote statistically significant differences between microhabitat means

(Continued on next page)

Fig 4 (Continued)

by Kruskal-Wallis non-parametric analysis of variance followed by Dunn's *post hoc* test (individual *P*-values <0.05; BH corrected). (C) Nonmetric multidimensional scaling computed using a Bray-Curtis dissimilarity matrix on functional genes. Individual shapes depict replicates of the indicated microhabitats, color-coded according to sample type or genotype. The R^2 value depicts the proportion of variation in distances explained by the factor microhabitat (adonis test, asterisks denote *P*-value <0.001; 5,000 permutations). (D) Cumulative abundance of genes representative of 15 most dominant functional categories enriched in and differentiating between rhizosphere and bulk soil in both genotypes (Wald test, individual *P*-values <0.05, FDR corrected).

databases, with the exception of the identification of an antibiotic efflux pump, *AbaQ*, previously implicated in quinolone resistance (63).

Finally, to gain further insights into the functional potential of the tomato microbiota, we expanded our investigation to eight additional MAGs (Table S5). With the caveat that these MAGs represent taxa whose abundance is at least an order of magnitude less than *Acinetobacter*, their enriched functions allowed us to identify three main categories, that is, Metabolism, Environmental Information, and Genetic Information Processing, displaying a "microhabitat" effect in both genotypes (Wald test, individual *P*-values <0.05, FDR corrected; see Data Set S5 at https://zenodo.org/records/17580416).

DISCUSSION

Similar to what was previously reported, the tomato plants grown in this "lab-in-the-field" hosted a bacterial community whose richness and diversity decrease from the unplanted soil to the inner root tissues, and communities are dominated by relatively few taxa (18).

A striking feature of our investigation is the dominance of an individual *Acinetobacter* sp. of the rhizosphere and root profiles. This dominance has previously been reported for tomato growing both in glasshouse (64) and field trials (65), and *Acinetobacter* can be isolated from tomato plants (66). This motivated us to discern the origin and functional significance of the observed dominance. For instance, it is known that exogenous factors may act as a reservoir for the tomato microbiota, as reported for rain and the phyllosphere microbiota (67). However, we found no evidence for a passive flow-through of *Acinetobacter* from the microbiota retrieved from different farm machinery. An alternative scenario is represented by the opportunistic nature of *Acinetobacter* colonization, as previously reported for *Ralstonia*-infected tomato plants (68). However, no evidence for disease establishment was reported for the investigated field. This left us with two plausible explanations. The first one is a seed transmission of microbes to mature plants, a scenario congruent with what was reported for beneficial bacteria inhabiting tomato inner tissues (69). The second explanation is represented by an enrichment from the surrounding soil biota of *Acinetobacter*. This latter explanation would be congruent with what we previously reported for field-grown tomato plants in the north of Italy (19). Time-course experiments, profiling the development of the tomato microbiota from seeds to transplanted seedlings to established crops, will be required to validate either (or both) scenarios.

As *Acinetobacter* dominance defines both belowground tomato microhabitats, we reasoned that a comparative metagenomic analysis of the rhizosphere and unplanted soil specimens would have provided us with insights into the biological significance of the bacterial enrichment. Consistently, the taxonomic composition of the obtained metagenomes reflected (i) the substantial congruence between the data obtained with different sequencing strategies and (ii) a bacterial dominance. This motivated us to infer functional significance using a two-pronged approach. First, we looked at the differential enrichment of a curated data set of plant-growth promoting functions (51), and we observed how mineral mobilization, including iron, phosphorus, and sulfur emerged as the dominant functions enriched in the tomato rhizosphere in a genotype-dependent manner. Other striking enrichments were represented by the adaptation to salinity and osmotic stresses, as well as detoxification of reactive oxygen species, as those processes are intertwined (70). As salinization is a developing threat for agricultural production in

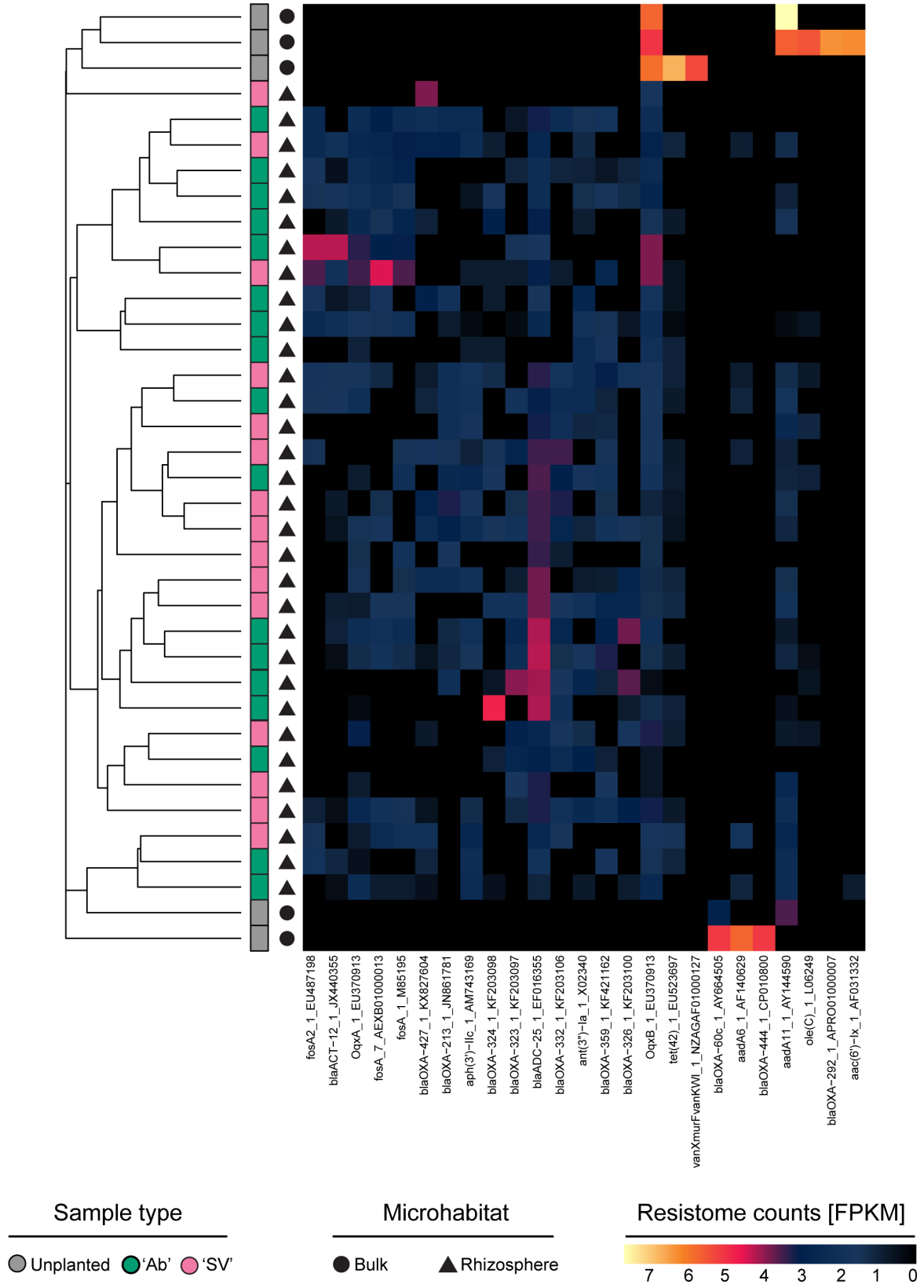

FIG 5 Abundance of individual ARGs, identified in the indicated microhabitats and tomato genotypes. Abbreviations: *fos*, fosfomycin resistance genes; *bla*, beta-lactamase; *Oqx*, efflux pumps, fluoroquinolone; *aph*, aminoglycoside 3′-phosphotransferase; *ant*, aminoglycoside nucleotidyltransferase; *tet*, tetracycline resistance genes; *aadA*, aminoglycoside adenylyltransferase; *oleC*, oleandomycin; *aaC*, aminoglycoside acetyltransferase.

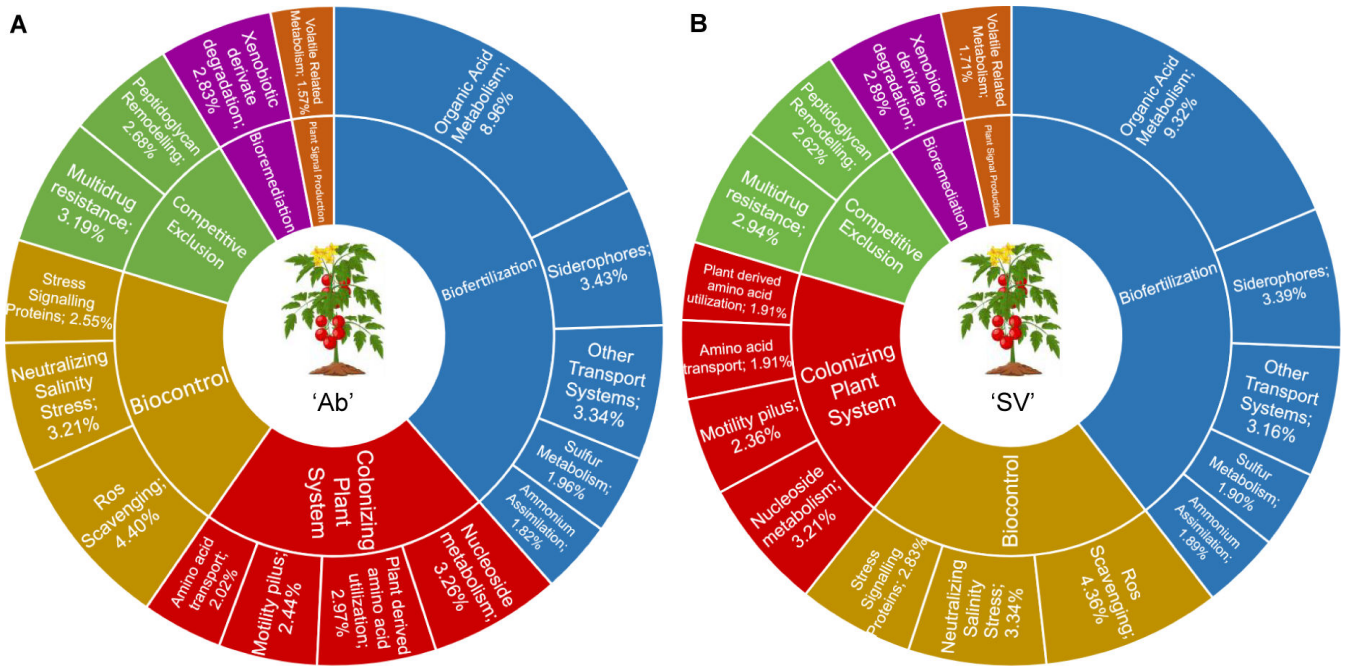

FIG 6 Average proportions of the most representative gene abundances associated with PGPT categories at level four, based on metagenomic reads assigned to *Acinetobacter calcoaceticus* in (A) "Ab" and (B) "SV" genotypes.

Mediterranean environments (71), these enrichments can be interpreted as evidence of the impact of climatic modifications on the tomato microbiota.

Taken together, these observations are congruent with the recruitment of a versatile plant growth-microbe at the tomato root-soil interface, fitting the profile of soil-borne *Acinetobacter* (72). Yet, although beneficial for their host, this recruitment may be a Janus-faced one. For instance, the genus *Acinetobacter* has been of clinical interest for decades (73), with *Acinetobacter baumannii* considered a paradigmatic example for its vast multidrug resistance capabilities (74). Alongside this established case study, other members of the genus are gaining center stage for their antimicrobial resistance (75, 76). For instance, naturally abundant *Acinetobacter* sp. in plant food chains may act as a vehicle for ARGs distribution in clinical settings (77), although "non-human" strains tend to have fewer antibiotic resistance genes, mostly intrinsic in nature (78). Consistently, we failed to obtain evidence that the beta-lactamase dominance identified in the community resistome links taxonomic composition with ARG distribution in the tomato microbiota, as previously reported across soil habitats (79). Although the genus *Acinetobacter* as a whole is recognized as a natural reservoir of beta-lactamase (80, 81), our results concur with a recent investigation of non-clinical isolates of *A. baumannii* from grasslands displaying a limited beta-lactamase distribution (coupled though with the presence of *AbaQ*) (82). Consequently, if ARGs confer an adaptive advantage to *Acinetobacter* colonization, this appears (i) habitat-specific, as we did not observe any enrichment for this bacterium in the phyllosphere, and (ii) decoupled from the "community resistome," that are ARGs coded by other members of the community. This result is aligned with previous observations (83) indicating that the soil resistome appears driven by abiotic factors, including temperature and precipitation, as opposed to the phyllosphere resistome responding to inter-microbial competition.

Our work suggests a scenario whereby the rhizosphere enrichment of a plant-beneficial bacterium is mediated, at least in part, by ARGs. Though drought tolerance is often associated with members of the phylum Actinobacteria (84), a recent investigation identified an *Acinetobacter* from arid soils among bacteria capable of alleviating tomato drought stress (85). It is therefore tempting to speculate that the observed

Acinetobacter enrichment may represent a "plant's attempt" at future-proofing the microbiota for better adaptation to climatic modifications. This scenario is reminiscent of the Pseudomonads phylotype "bloom" occurring in a host genotype-independent manner in the sorghum microbiota (86): dominant phylotypes, unlike "hubs," respond rapidly to substrate- and/or environmental-driven fluctuations and may establish with poor connectivity with the rest of the microbiota. With increased knowledge of the host genetic determinants of the tomato microbiota (15), beneficial microbial enrichment could be soon integrated into plant breeding strategies (3). In doing so, it will, however, be important to consider potential trade-offs between microbial configurations and tomato performance, as highlighted by both ecological (87) and molecular (88) investigations. This may include the characterization of isolates of the identified *Acinetobacter*, complementing surveys envisioned for the genera (89) and/or for other plant growth-promoting bacteria (90). In turn, this will provide scientists and practitioners with a better understanding of the "One Health impact" of the deliberate manipulation of individual members of the plant microbiota.

A limitation of the study is that we report the results of an individual year of experimentation from an individual farm. As plant development is known to fine-tune the recruitment cues of the microbiota, as previously reported by ourselves (19) and other groups (91), the individual experiment prevented us from inferring the contribution of season-to-season variation in shaping the tomato microbiota. Further experimentations, across growing seasons and farms, will elucidate the deterministic nature of microhabitat and host genetic factors in defining composition and function of the microbiota thriving in association with field-grown plants.

ACKNOWLEDGMENTS

This work was supported by the Horizon 2020 Framework Programme Innovation Action "CIRCLES" (European Commission grant agreement 818290) awarded to the University of Dundee, the University of Bologna, the Luxembourg Centre for Systems Biomedicine, DTU, and MS Biotech. C.A. is supported by a UKRI BBSRC eastBIO PhD studentship (project 2734186).

We are thankful to the farmers who provided us with access to their fields. We thank Elena Del Rio and Jennifer Gallagher (University of Dundee) for their administrative and technical support, respectively, in delivering the project.

AUTHOR AFFILIATIONS

[1]Plant Sciences, School of Life Sciences, University of Dundee, Dundee, United Kingdom
[2]Computational Biology, School of Life Sciences, University of Dundee, Dundee, United Kingdom
[3]Department of Agriculture, Food and Environment, University of Catania, Catania, Italy
[4]Cell and Molecular Sciences, The James Hutton Institute, Dundee, United Kingdom
[5]Department of Pharmacy and Biotechnology, University of Bologna, Bologna, Italy
[6]Research Group for Genomic Epidemiology, National Food Institute, Technical University of Denmark, Lyngby, Denmark
[7]Luxembourg Centre for Systems Biomedicine, University of Luxembourg, Esch-sur-Alzette, Luxembourg
[8]Department of Life Sciences and Medicine, University of Luxembourg, Esch-sur-Alzette, Luxembourg
[9]MS Biotech, Larino, Campobasso, Italy

PRESENT ADDRESS

Senga Robertson, School of Health Science, University of Dundee, Dundee, United Kingdom
Rodrigo Alegria Terrazas, Rothamsted Research, Harpenden, United Kingdom

AUTHOR ORCIDs

Senga Robertson http://orcid.org/0000-0001-5907-714X
Alexandros Mosca http://orcid.org/0000-0001-8352-8457
Rodrigo Alegria Terrazas http://orcid.org/0000-0002-3005-7273
Catherine Arnton http://orcid.org/0009-0001-2775-8060
Peter Thorpe http://orcid.org/0000-0001-8572-4654
Giulia Babbi http://orcid.org/0000-0002-9816-4737
Castrense Savojardo http://orcid.org/0000-0002-7359-0633
Pier Luigi Martelli http://orcid.org/0000-0002-0274-5669
Frederik Duus Møller http://orcid.org/0000-0003-0655-1551
Hanne Nørgaard Nielsen http://orcid.org/0009-0005-7327-0241
Pimlapas Leekitcharoenphon http://orcid.org/0000-0002-5674-0142
Frank M. Aarestrup http://orcid.org/0000-0002-7116-2723
Cedric C. Laczny http://orcid.org/0000-0002-1100-1282
Paul Wilmes http://orcid.org/0000-0002-6478-2924
Vittoria Catara http://orcid.org/0000-0001-8076-258X
James Abbott http://orcid.org/0000-0001-7701-4249
Davide Bulgarelli http://orcid.org/0000-0002-2020-6642

FUNDING

Funder	Grant(s)	Author(s)
Horizon 2020 Framework Programme	818290	Senga Robertson Saira Ashraf Aileen Corral Rodrigo Alegria Terrazas Giulia Babbi Castrense Savojardo Pier Luigi Martelli Frederik Duus Møller Hanne Nørgaard Nielsen Pimlapas Leekitcharoenphon Frank M. Aarestrup Rashi Halder Cedric C. Laczny Paul Wilmes Laura Pietrantonio Pardo Di Cillo Davide Bulgarelli
Biotechnology and Biological Sciences Research Council	2734186	Davide Bulgarelli

AUTHOR CONTRIBUTIONS

Senga Robertson, Conceptualization, Data curation, Formal analysis, Investigation, Project administration, Visualization, Writing – original draft, Writing – review and editing | Alexandros Mosca, Conceptualization, Data curation, Formal analysis, Methodology, Visualization, Writing – original draft, Writing – review and editing | Saira Ashraf, Investigation, Methodology, Writing – review and editing | Aileen Corral, Investigation, Methodology, Writing – review and editing | Rodrigo Alegria Terrazas, Investigation, Writing – review and editing | Catherine Arnton, Formal analysis, Visualization, Writing

– review and editing | Peter Thorpe, Data curation, Formal analysis, Writing – review and editing | Jenny Morris, Methodology, Resources, Writing – review and editing | Pete E. Hedley, Methodology, Resources, Writing – review and editing | Giulia Babbi, Data curation, Formal analysis, Writing – review and editing | Castrense Savojardo, Resources, Writing – review and editing | Pier Luigi Martelli, Data curation, Formal analysis, Funding acquisition, Supervision, Writing – review and editing | Frederik Duus Møller, Data curation, Formal analysis, Visualization, Writing – review and editing | Hanne Nørgaard Nielsen, Methodology, Writing – review and editing | Pimlapas Leekitcharoenphon, Data curation, Formal analysis, Visualization, Writing – review and editing | Frank M. Aarestrup, Funding acquisition, Project administration, Supervision, Writing – review and editing | Rashi Halder, Investigation, Methodology, Writing – review and editing | Cedric C. Laczny, Investigation, Methodology, Supervision, Writing – review and editing | Paul Wilmes, Funding acquisition, Project administration, Supervision, Writing – review and editing | Laura Pietrantonio, Investigation, Writing – review and editing | Pardo Di Cillo, Funding acquisition, Investigation, Project administration, Writing – review and editing | Vittoria Catara, Supervision, Writing – review and editing | James Abbott, Conceptualization, Data curation, Formal analysis, Methodology, Supervision, Writing – review and editing | Davide Bulgarelli, Conceptualization, Data curation, Formal analysis, Funding acquisition, Project administration, Supervision, Validation, Writing – original draft, Writing – review and editing

DATA AVAILABILITY

The genomic sequences reported in this study are deposited in the European Nucleotide Archive (ENA), project PRJEB80388. The codes to reproduce data analyses are available at https://github.com/BulgarelliD-Lab/CIRCLES_Tomato.

ADDITIONAL FILES

The following material is available online.

Supplemental Material

Supplemental Material (mSphere00842-25-S0001.docx). Tables S1 to S5; Fig. S1 to S8.

REFERENCES

1. Bulgarelli D, Schlaeppi K, Spaepen S, Ver Loren van Themaat E, Schulze-Lefert P. 2013. Structure and functions of the bacterial microbiota of plants. Annu Rev Plant Biol 64:807–838. https://doi.org/10.1146/annurev-arplant-050312-120106
2. van Bruggen AHC, Goss EM, Havelaar A, van Diepeningen AD, Finckh MR, Morris JG Jr. 2019. One Health - Cycling of diverse microbial communities as a connecting force for soil, plant, animal, human and ecosystem health. Sci Total Environ 664:927–937. https://doi.org/10.1016/j.scitotenv.2019.02.091
3. Escudero-Martinez C, Bulgarelli D. 2023. Engineering the crop microbiota through host genetics. Annu Rev Phytopathol 61:257–277. https://doi.org/10.1146/annurev-phyto-021621-121447
4. Schlaeppi K, Bulgarelli D. 2015. The plant microbiome at work. Mol Plant Microbe Interact 28:212–217. https://doi.org/10.1094/MPMI-10-14-0334-FI
5. Chen Q-L, Cui H-L, Su J-Q, Penuelas J, Zhu Y-G. 2019. Antibiotic resistomes in plant microbiomes. Trends Plant Sci 24:530–541. https://doi.org/10.1016/j.tplants.2019.02.010
6. Cernava T, Erlacher A, Soh J, Sensen CW, Grube M, Berg G. 2019. *Enterobacteriaceae* dominate the core microbiome and contribute to the resistome of arugula (*Eruca sativa* Mill.). Microbiome 7:13. https://doi.org/10.1186/s40168-019-0624-7
7. Obermeier MM, Wicaksono WA, Taffner J, Bergna A, Poehlein A, Cernava T, Lindstaedt S, Lovric M, Müller Bogotá CA, Berg G. 2021. Plant resistome profiling in evolutionary old bog vegetation provides new clues to understand emergence of multi-resistance. ISME J 15:921–937. https://doi.org/10.1038/s41396-020-00822-9
8. Berg G, Cernava T. 2022. The plant microbiota signature of the Anthropocene as a challenge for microbiome research. Microbiome 10:54. https://doi.org/10.1186/s40168-021-01224-5
9. Banerjee S, van der Heijden MGA. 2023. Soil microbiomes and one health. Nat Rev Microbiol 21:6–20. https://doi.org/10.1038/s41579-022-00779-w
10. Fernie AR, Yan J. 2019. *De novo* domestication: an alternative route toward new crops for the future. Mol Plant 12:615–631. https://doi.org/10.1016/j.molp.2019.03.016
11. Wang Y, Sun C, Ye Z, Li C, Huang S, Lin T. 2024. The genomic route to tomato breeding: past, present, and future. Plant Physiol 195:2500–2514. https://doi.org/10.1093/plphys/kiae248
12. Cammarano D, Jamshidi S, Hoogenboom G, Ruane AC, Niyogi D, Ronga D. 2022. Processing tomato production is expected to decrease by 2050 due to the projected increase in temperature. Nat Food 3:437–444. https://doi.org/10.1038/s43016-022-00521-y
13. Zsögön A, Čermák T, Naves ER, Notini MM, Edel KH, Weinl S, Freschi L, Voytas DF, Kudla J, Peres LEP. 2018. *De novo* domestication of wild tomato using genome editing. Nat Biotechnol 36:1211–1216. https://doi.org/10.1038/nbt.4272
14. George TS, Bulgarelli D, Carminati A, Chen Y, Jones D, Kuzyakov Y, Schnepf A, Wissuwa M, Roose T. 2024. Bottom-up perspective - The role of roots and rhizosphere in climate change adaptation and mitigation in agroecosystems. Plant Soil 500:297–323. https://doi.org/10.1007/s11104-024-06626-6
15. Oyserman BO, Flores SS, Griffioen T, Pan X, van der Wijk E, Pronk L, Lokhorst W, Nurfikari A, Paulson JN, Movassagh M, Stopnisek N, Kupczok

A, Cordovez V, Carrión VJ, Ligterink W, Snoek BL, Medema MH, Raaijmakers JM. 2022. Disentangling the genetic basis of rhizosphere microbiome assembly in tomato. Nat Commun 13:3228. https://doi.org/10.1038/s41467-022-30849-9
16. Kwak M-J, Kong HG, Choi K, Kwon S-K, Song JY, Lee J, Lee PA, Choi SY, Seo M, Lee HJ, Jung EJ, Park H, Roy N, Kim H, Lee MM, Rubin EM, Lee S-W, Kim JF. 2018. Rhizosphere microbiome structure alters to enable wilt resistance in tomato. Nat Biotechnol 36:1100–1109. https://doi.org/10.1038/nbt.4232
17. Lee S-M, Kong HG, Song GC, Ryu C-M. 2021. Disruption of Firmicutes and Actinobacteria abundance in tomato rhizosphere causes the incidence of bacterial wilt disease. ISME J 15:330–347. https://doi.org/10.1038/s41396-020-00785-x
18. Flores SS, CordovezV, Oyserman B, Stopnisek N, Raaijmakers JM, van't Hof P. 2023. The tomato's tale: exploring taxonomy, biogeography, domestication, and microbiome for enhanced resilience. Phytobiomes J 8:5–20. https://doi.org/10.1094/PBIOMES-09-23-0091-MF
19. Caradonia F, Ronga D, Catellani M, Giaretta Azevedo CV, Terrazas RA, Robertson-Albertyn S, Francia E, Bulgarelli D. 2019. Nitrogen fertilizers shape the composition and predicted functions of the microbiota of field-grown tomato plants. Phytobiomes J 3:315–325. https://doi.org/10.1094/PBIOMES-06-19-0028-R
20. Talavera-Marcos S, Gallego R, Chaboy-Cansado R, Rastrojo A, Aguirre de Cárcer D. 2025. Coupled phylogenetic and functional enrichment in the tomato rhizosphere microbiome. Phytobiomes J 9:151–156. https://doi.org/10.1094/PBIOMES-10-24-0098-SC
21. Li Y, Lei S, Cheng Z, Jin L, Zhang T, Liang L-M, Cheng L, Zhang Q, Xu X, Lan C, Lu C, Mo M, Zhang K-Q, Xu J, Tian B. 2023. Microbiota and functional analyses of nitrogen-fixing bacteria in root-knot nematode parasitism of plants. Microbiome 11:48. https://doi.org/10.1186/s40168-023-01484-3
22. Barajas HR, Martínez-Sánchez S, Romero MF, Álvarez CH, Servín-González L, Peimbert M, Cruz-Ortega R, García-Oliva F, Alcaraz LD. 2020. Testing the two-step model of plant root microbiome acquisition under multiple plant species and soil sources. Front Microbiol 11:542742. https://doi.org/10.3389/fmicb.2020.542742
23. Gilbert JA, Jansson JK, Knight R. 2018. Earth microbiome project and global systems biology. mSystems 3:e00217-17. https://doi.org/10.1128/mSystems.00217-17
24. Lundberg DS, Yourstone S, Mieczkowski P, Jones CD, Dangl JL. 2013. Practical innovations for high-throughput amplicon sequencing. Nat Methods 10:999–1002. https://doi.org/10.1038/nmeth.2634
25. Scicchitano D, Leuzzi D, Babbi G, Palladino G, Turroni S, Laczny CC, Wilmes P, Correa F, Leekitcharoenphon P, Savojardo C, Luise D, Martelli P, Trevisi P, Aarestrup FM, Candela M, Rampelli S. 2024. Dispersion of antimicrobial resistant bacteria in pig farms and in the surrounding environment. Anim Microbiome 6:17. https://doi.org/10.1186/s42523-024-00305-8
26. Maver M, Escudero-Martinez C, Abbott J, Morris J, Hedley PE, Mimmo T, Bulgarelli D. 2021. Applications of the indole-alkaloid gramine modulate the assembly of individual members of the barley rhizosphere microbiota. PeerJ 9:e12498. https://doi.org/10.7717/peerj.12498
27. McMurdie PJ, Holmes S. 2013. phyloseq: an R package for reproducible interactive analysis and graphics of microbiome census data. PLoS One 8:e61217. https://doi.org/10.1371/journal.pone.0061217
28. Pietrangelo L, Bucci A, Maiuro L, Bulgarelli D, Naclerio G. 2018. Unraveling the composition of the root-associated bacterial microbiota of *Phragmites australis* and *Typha latifolia*. Front Microbiol 9:1650. https://doi.org/10.3389/fmicb.2018.01650
29. Bokulich NA, Subramanian S, Faith JJ, Gevers D, Gordon JI, Knight R, Mills DA, Caporaso JG. 2013. Quality-filtering vastly improves diversity estimates from Illumina amplicon sequencing. Nat Methods 10:57–59. https://doi.org/10.1038/nmeth.2276
30. Selten G, Lamouche F, Gomez-Repolles A, Blahovska Z, Kelly S, de Jonge R, Radutoiu S. 2024. Functional capacities drive recruitment of bacteria into plant root microbiota. bioRxiv. https://doi.org/10.1101/2024.08.22.609090
31. Oksanen J, Kindt R, Legendre P, O'Hara B, Stevens MHH, Oksanen MJ, Suggests M. 2007. The vegan package. Community ecology package
32. Love MI, Huber W, Anders S. 2014. Moderated estimation of fold change and dispersion for RNA-seq data with DESeq2. Genome Biol 15:550. https://doi.org/10.1186/s13059-014-0550-8
33. Friedman J, Alm EJ. 2012. Inferring correlation networks from genomic survey data. PLoS Comput Biol 8:e1002687. https://doi.org/10.1371/journal.pcbi.1002687
34. Shannon P, Markiel A, Ozier O, Baliga NS, Wang JT, Ramage D, Amin N, Schwikowski B, Ideker T. 2003. Cytoscape: a software environment for integrated models of biomolecular interaction networks. Genome Res 13:2498–2504. https://doi.org/10.1101/gr.1239303
35. Su G, Kuchinsky A, Morris JH, States DJ, Meng F. 2010. GLay: community structure analysis of biological networks. Bioinformatics 26:3135–3137. https://doi.org/10.1093/bioinformatics/btq596
36. Doncheva NT, Assenov Y, Domingues FS, Albrecht M. 2012. Topological analysis and interactive visualization of biological networks and protein structures. Nat Protoc 7:670–685. https://doi.org/10.1038/nprot.2012.004
37. Krueger F, James F, Ewels P, Afyounian E, Schuster-Boeckler BT. 2016. A wrapper around Cutadapt and FastQC to consistently apply adapter and quality trimming to FastQ files, with extra functionality for RRBS data. TrimGalore. Retrieved 27 Aug 2019.
38. Wood DE, Lu J, Langmead B. 2019. Improved metagenomic analysis with Kraken 2. Genome Biol 20:257. https://doi.org/10.1186/s13059-019-1891-0
39. Li H. 2013. Aligning sequence reads, clone sequences and assembly contigs with BWA-MEM. arXiv. https://doi.org/10.48550/arXiv.1303.3997
40. Li H, Handsaker B, Wysoker A, Fennell T, Ruan J, Homer N, Marth G, Abecasis G, Durbin R, Subgroup GPDP. 2009. The sequence alignment/map format and SAMtools. Bioinformatics 25:2078–2079. https://doi.org/10.1093/bioinformatics/btp352
41. Li D, Liu C-M, Luo R, Sadakane K, Lam T-W. 2015. MEGAHIT: an ultra-fast single-node solution for large and complex metagenomics assembly via succinct de Bruijn graph. Bioinformatics 31:1674–1676. https://doi.org/10.1093/bioinformatics/btv033
42. Kang DD, Li F, Kirton E, Thomas A, Egan R, An H, Wang Z. 2019. MetaBAT 2: an adaptive binning algorithm for robust and efficient genome reconstruction from metagenome assemblies. PeerJ 7:e7359. https://doi.org/10.7717/peerj.7359
43. Olm MR, Brown CT, Brooks B, Banfield JF. 2017. dRep: a tool for fast and accurate genomic comparisons that enables improved genome recovery from metagenomes through de-replication. ISME J 11:2864–2868. https://doi.org/10.1038/ismej.2017.126
44. Nayfach S, Shi ZJ, Seshadri R, Pollard KS, Kyrpides NC. 2019. New insights from uncultivated genomes of the global human gut microbiome. Nature 568:505–510. https://doi.org/10.1038/s41586-019-1058-x
45. Parks DH, Imelfort M, Skennerton CT, Hugenholtz P, Tyson GW. 2015. CheckM: assessing the quality of microbial genomes recovered from isolates, single cells, and metagenomes. Genome Res 25:1043–1055. https://doi.org/10.1101/gr.186072.114
46. Schwengers O, Jelonek L, Dieckmann MA, Beyvers S, Blom J, Goesmann A. 2021. Bakta: rapid and standardized annotation of bacterial genomes via alignment-free sequence identification. Microb Genom 7:000685. https://doi.org/10.1099/mgen.0.000685
47. Chaumeil P-A, Mussig AJ, Hugenholtz P, Parks DH. 2020. GTDB-Tk: a toolkit to classify genomes with the Genome Taxonomy Database. Bioinformatics 36:1925–1927. https://doi.org/10.1093/bioinformatics/btz848
48. Jain C, Rodriguez-R LM, Phillippy AM, Konstantinidis KT, Aluru S. 2018. High throughput ANI analysis of 90K prokaryotic genomes reveals clear species boundaries. Nat Commun 9:5114. https://doi.org/10.1038/s41467-018-07641-9
49. Grant JR, Enns E, Marinier E, Mandal A, Herman EK, Chen C-Y, Graham M, Van Domselaar G, Stothard P. 2023. Proksee: in-depth characterization and visualization of bacterial genomes. Nucleic Acids Res 51:W484–W492. https://doi.org/10.1093/nar/gkad326
50. Pellegrinetti TA, Monteiro GGTN, Lemos LN, Santos RAC dos, Barros AG, Mendes LW. 2024. PGPg_finder: a comprehensive and user-friendly pipeline for identifying plant growth-promoting genes in genomic and metagenomic data. Rhizosphere 30:100905. https://doi.org/10.1016/j.rhisph.2024.100905
51. Patz S, Gautam A, Becker M, Ruppel S, Rodríguez-Palenzuela P, Huson D. 2021. PLaBAse: a comprehensive web resource for analyzing the plant growth-promoting potential of plant-associated bacteria. bioRxiv. https://doi.org/10.1101/2021.12.13.472471

52. Cantalapiedra CP, Hernández-Plaza A, Letunic I, Bork P, Huerta-Cepas J. 2021. eggNOG-mapper v2: functional annotation, orthology assignments, and domain prediction at the metagenomic scale. Mol Biol Evol 38:5825–5829. https://doi.org/10.1093/molbev/msab293
53. Bortolaia V, Kaas RS, Ruppe E, Roberts MC, Schwarz S, Cattoir V, Philippon A, Allesoe RL, Rebelo AR, Florensa AF, et al. 2020. ResFinder 4.0 for predictions of phenotypes from genotypes. J Antimicrob Chemother 75:3491–3500. https://doi.org/10.1093/jac/dkaa345
54. Clausen PTLC, Aarestrup FM, Lund O. 2018. Rapid and precise alignment of raw reads against redundant databases with KMA. BMC Bioinformatics 19:307. https://doi.org/10.1186/s12859-018-2336-6
55. Hendriksen RS, Munk P, Njage P, van Bunnik B, McNally L, Lukjancenko O, Röder T, Nieuwenhuijse D, Pedersen SK, Kjeldgaard J, et al. 2019. Global monitoring of antimicrobial resistance based on metagenomics analyses of urban sewage. Nat Commun 10:1124. https://doi.org/10.1038/s41467-019-08853-3
56. Zhao Y, Li M-C, Konaté MM, Chen L, Das B, Karlovich C, Williams PM, Evrard YA, Doroshow JH, McShane LM. 2021. TPM, FPKM, or normalized counts? A comparative study of quantification measures for the analysis of RNA-seq data from the NCI patient-derived models repository. J Transl Med 19:269. https://doi.org/10.1186/s12967-021-02936-w
57. Alcock BP, Huynh W, Chalil R, Smith KW, Raphenya AR, Wlodarski MA, Edalatmand A, Petkau A, Syed SA, Tsang KK, et al. 2023. CARD 2023: expanded curation, support for machine learning, and resistome prediction at the Comprehensive Antibiotic Resistance Database. Nucleic Acids Res 51:D690–D699. https://doi.org/10.1093/nar/gkac920
58. Pietrantonio L, Devers-Lamrani M, Thorpe P, Arnton C, Robertson-Albertyn S, Savojardo C, Hartmann A, Martin-Laurent F, Abbott J, Bulgarelli D. 2025. A genome-annotated bacterial collection of the plant food system microbiota. Microbiol Resour Announc 14:e0122124. https://doi.org/10.1128/mra.01221-24
59. Patz S, Rauh M, Gautam A, Huson DH. 2024. mgPGPT: metagenomic analysis of plant growth-promoting traits. bioRxiv. https://doi.org/10.1101/2024.02.17.580828
60. Achudhan AB, Saleena LM. 2024. Comparative genomic analysis and characterization of novel high-quality draft genomes from the coal metagenome. World J Microbiol Biotechnol 40:370. https://doi.org/10.1007/s11274-024-04174-w
61. Kimbrel JA, Thissen JB, Lisboa FA, Mabery S, Jaing CJ, Elster EA, Schobel SA, Be NA. 2025. High-quality *Acinetobacter* genomes recovered from combat wounds via metagenomic sequencing resemble cultured isolate genomes. Microbiol Spectr:e0187625. https://doi.org/10.1128/spectrum.01876-25
62. López-Sánchez R, Aguilar-Vera A, Castillo-Ramírez S. 2025. Metagenome-assembled genomes reveal novel diversity and atypical sources of a superbug. Microbiol Spectr 13:e0010625. https://doi.org/10.1128/spectrum.00106-25
63. Pérez-Varela M, Corral J, Aranda J, Barbé J. 2018. Functional characterization of AbaQ, a novel efflux pump mediating quinolone resistance in *Acinetobacter baumannii*. Antimicrob Agents Chemother 62:e00906-18. https://doi.org/10.1128/AAC.00906-18
64. Romero FM, Marina M, Pieckenstain FL. 2014. The communities of tomato (*Solanum lycopersicum* L.) leaf endophytic bacteria, analyzed by 16S-ribosomal RNA gene pyrosequencing. FEMS Microbiol Lett 351:187–194. https://doi.org/10.1111/1574-6968.12377
65. Dong C-J, Wang L-L, Li Q, Shang Q-M. 2019. Bacterial communities in the rhizosphere, phyllosphere and endosphere of tomato plants. PLoS One 14:e0223847. https://doi.org/10.1371/journal.pone.0223847
66. Muñoz CY, de Jong A, Kuipers OP. 2021. Draft genome sequences of a *Bacillus subtilis* strain, a *Bacillus velezensis* strain, a *Paenibacillus* strain, and an *Acinetobacter baumannii* strain, all isolated from the phyllosphere of *Lactuca sativa* or *Solanum lycopersicum*. Microbiol Resour Announc 10:e01092-20. https://doi.org/10.1128/MRA.01092-20
67. Mechan Llontop ME, Tian L, Sharma P, Heflin L, Bernal-Galeano V, Haak DC, Clarke CR, Vinatzer BA. 2021. Experimental evidence pointing to rain as a reservoir of tomato phyllosphere microbiota. Phytobiomes J 5:382–399. https://doi.org/10.1094/PBIOMES-04-21-0025-R
68. Kay E, Bertolla F, Vogel TM, Simonet P. 2002. Opportunistic colonization of *Ralstonia solanacearum*-infected plants by *Acinetobacter* sp. and its natural competence development. Microb Ecol 43:291–297. https://doi.org/10.1007/s00248-002-2007-y
69. Bergna A, Cernava T, Rändler M, Grosch R, Zachow C, Berg G. 2018. Tomato seeds preferably transmit plant beneficial endophytes. Phytobiomes J 2:183–193. https://doi.org/10.1094/PBIOMES-06-18-0029-R
70. Miller G, Suzuki N, Ciftci - yilmaz S, Mittler R. 2010. Reactive oxygen species homeostasis and signalling during drought and salinity stresses. Plant Cell Environ 33:453–467. https://doi.org/10.1111/j.1365-3040.2009.02041.x
71. Daliakopoulos IN, Tsanis IK, Koutroulis A, Kourgialas NN, Varouchakis AE, Karatzas GP, Ritsema CJ. 2016. The threat of soil salinity: a European scale review. Sci Total Environ 573:727–739. https://doi.org/10.1016/j.scitotenv.2016.08.177
72. Mujumdar S, Bhoyar J, Akkar A, Hundekar S, Agnihotri N, Jaybhay P, Bhuyan S. 2023. *Acinetobacter*: a versatile plant growth-promoting rhizobacteria (PGPR), p 327–362. In Plant-microbe interaction-recent advances in molecular and biochemical approaches. Elsevier.
73. Wong D, Nielsen TB, Bonomo RA, Pantapalangkoor P, Luna B, Spellberg B. 2017. Clinical and pathophysiological overview of *Acinetobacter* infections: a century of challenges. Clin Microbiol Rev 30:409–447. https://doi.org/10.1128/CMR.00058-16
74. Gootz TD, Marra A. 2008. *Acinetobacter baumannii*: an emerging multidrug-resistant threat. Expert Rev Anti Infect Ther 6:309–325. https://doi.org/10.1586/14787210.6.3.309
75. Aguilar-Vera A, Bello-López E, Pantoja-Nuñez GI, Rodríguez-López GM, Morales-Erasto V, Castillo-Ramírez S. 2024. *Acinetobacter junii*: an emerging One Health pathogen. mSphere 9:e0016224. https://doi.org/10.1128/msphere.00162-24
76. Castillo-Ramírez S, Mateo-Estrada V, Gonzalez-Rocha G, Opazo-Capurro A. 2020. Phylogeographical analyses and antibiotic resistance genes of *Acinetobacter johnsonii* highlight its clinical relevance. mSphere 5:e00581-20. https://doi.org/10.1128/mSphere.00581-20
77. Berlau J, Aucken HM, Houang E, Pitt TL. 1999. Isolation of *Acinetobacter* spp. including *A. baumannii* from vegetables: implications for hospital-acquired infections. J Hosp Infect 42:201–204. https://doi.org/10.1053/jhin.1999.0602
78. Castillo-Ramírez S, Aguilar-Vera A, Kumar A, Evans B. 2025. *Acinetobacter baumannii*: much more than a human pathogen. Antimicrob Agents Chemother 69:e0080125. https://doi.org/10.1128/aac.00801-25
79. Forsberg KJ, Patel S, Gibson MK, Lauber CL, Knight R, Fierer N, Dantas G. 2014. Bacterial phylogeny structures soil resistomes across habitats. Nature 509:612–616. https://doi.org/10.1038/nature13377
80. Migliaccio A, Bray J, Intoccia M, Stabile M, Scala G, Jolley KA, Brisse S, Zarrilli R. 2023. Phylogenomics of *Acinetobacter* species and analysis of antimicrobial resistance genes. Front Microbiol 14:1264030. https://doi.org/10.3389/fmicb.2023.1264030
81. Zhao W-H, Hu Z-Q. 2012. *Acinetobacter*: a potential reservoir and dispenser for β-lactamases. Crit Rev Microbiol 38:30–51. https://doi.org/10.3109/1040841X.2011.621064
82. Mateo-Estrada V, Tyrrell C, Evans BA, Aguilar-Vera A, Drissner D, Castillo-Ramirez S, Walsh F. 2023. *Acinetobacter baumannii* from grass: novel but non-resistant clones. Microb Genom 9:001054. https://doi.org/10.1099/mgen.0.001054
83. Yan Z-Z, Chen Q-L, Li C-Y, Thi Nguyen B-A, Zhu Y-G, He J-Z, Hu H-W. 2021. Biotic and abiotic factors distinctly drive contrasting biogeographic patterns between phyllosphere and soil resistomes in natural ecosystems. ISME Commun 1:13. https://doi.org/10.1038/s43705-021-00012-4
84. Ebrahimi-Zarandi M, Etesami H, Glick BR. 2023. Fostering plant resilience to drought with Actinobacteria: unveiling perennial allies in drought stress tolerance. Plant Stress 10:100242. https://doi.org/10.1016/j.stress.2023.100242
85. Schmitz L, Yan Z, Schneijderberg M, de Roij M, Pijnenburg R, Zheng Q, Franken C, Dechesne A, Trindade LM, van Velzen R, Bisseling T, Geurts R, Cheng X. 2022. Synthetic bacterial community derived from a desert rhizosphere confers salt stress resilience to tomato in the presence of a soil microbiome. ISME J 16:1907–1920. https://doi.org/10.1038/s41396-022-01238-3
86. Chiniquy D, Barnes EM, Zhou J, Hartman K, Li X, Sheflin A, Pella A, Marsh E, Prenni J, Deutschbauer AM, Schachtman DP, Tringe SG. 2021. Microbial community field surveys reveal abundant *Pseudomonas* population in sorghum rhizosphere composed of many closely related phylotypes. Front Microbiol 12:598180. https://doi.org/10.3389/fmicb.2021.598180
87. Carrillo J, Ingwell LL, Li X, Kaplan I. 2019. Domesticated tomatoes are more vulnerable to negative plant–soil feedbacks than their wild relatives. J Ecol 107:1753–1766. https://doi.org/10.1111/1365-2745.13157

88. Chialva M, Salvioli di Fossalunga A, Daghino S, Ghignone S, Bagnaresi P, Chiapello M, Novero M, Spadaro D, Perotto S, Bonfante P. 2018. Native soils with their microbiotas elicit a state of alert in tomato plants. New Phytol 220:1296–1308. https://doi.org/10.1111/nph.15014
89. Hernández-González IL, Castillo-Ramírez S. 2020. Antibiotic-resistant *Acinetobacter baumannii* is a One Health problem. Lancet Microbe 1:e279. https://doi.org/10.1016/S2666-5247(20)30167-1
90. Bellotti G, Cortimiglia C, Antinori ME, Cocconcelli PS, Puglisi E. 2025. Comprehensive genome-wide analysis for the safety assessment of microbial biostimulants in agricultural applications. Microb Genom 11:001391. https://doi.org/10.1099/mgen.0.001391
91. Dong M, Kuramae EE, Zhao M, Li R, Shen Q, Kowalchuk GA. 2023. Tomato growth stage modulates bacterial communities across different soil aggregate sizes and disease levels. ISME Commun 3:104. https://doi.org/10.1038/s43705-023-00312-x